Pure Appl. Chem., Vol. 77, No. 10, pp. 1685–1706, 2005.
DOI: 10.1351/pac200577101685

Binuclear complexes as tectons in designing supramolecular solid-state architectures*,**

Marius Andruh

Faculty of Chemistry, Inorganic Chemistry Laboratory, University of Bucharest, Str. Dumbrava Rosie nr. 23, 020464-Bucharest, Romania

Abstract: Oligonuclear complexes as well as coordination polymers with various network topologies can be obtained by using homo- or heterobinuclear complexes as starting materials. These building blocks are stable complexes, where the metal ions are held together by compartmental ligands, or alkoxo-bridged Cu(II) species. The binuclear nodes can be connected through appropriate *exo*-dentate ligands, or through metal-containing anions (e.g., $[M(CN)_6]^{3-}$, M = Cr^{III}, Fe^{III}, Co^{III}). A rich variety of 3d-3d and 3d-4f heterometallic complexes, with interesting architectures and topologies of the spin carriers, has been obtained. A particular case is the one concerning the 3d-4f binuclear nodes. Following this strategy, we were able to obtain coordination polymers containing three different spin carriers (2p-3d-4f; 3d-3d'-4f).

Keywords: Crystal engineering; molecular magnetism; lanthanide complexes; Cu(II) complexes; tetranuclear complexes.

INTRODUCTION

The search for new synthetic routes leading to multimetallic complexes is of current interest in inorganic chemistry [1]. The building block approach was particularly developed in order to obtain heterometallic complexes with interesting magnetic, optical, electric, or catalytic properties. It consists of the use of anionic complexes, with potentially bridging ligands (linkers), which may interact with a wide variety of assembling cations (connectors), Scheme 1. An extremely rich chemistry has been developed, particularly with the families of oxamido [2], cyano- [3], and oxalato-bridged systems [4]. Paralleling the rational way of metal assembling, the serendipitous assembly also affords compounds with spectacular structures and properties [5]. The retrospective analysis of the compounds obtained by accident provides the necessary information in the attempt to design complexes with pre-established nuclearities and dimensionalities.

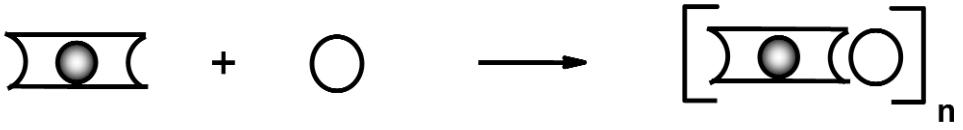

Scheme 1

*Paper based on a presentation at the 4th International Conference of the Chemical Societies of the South-Eastern European Countries (ICOSECS-4), Belgrade, Serbia and Montenegro, 18–21 July 2004. Other presentations are published in this issue, pp. 1655–1752.

**Dedicated to Prof. Herbert W. Roesky on the occasion of his 70th birthday.

We are currently developing a synthetic approach aimed at obtaining multimetallic complexes by using homo- and heterobinuclear complexes as building blocks (Scheme 2). The following types of cationic species are employed as connectors: (i) alkoxo-bridged Cu(II) species; (ii) binuclear Cu(II) species with end-off compartmental Schiff-base ligands; (iii) binuclear Cu(II) complexes with macrocyclic Robson ligands; (iv) heterobinuclear 3d-4f species with side-off Schiff-base ligands (Scheme 3). Various ligands can be used as linkers: neutral organic molecules, anionic organic species, and anionic complexes with potentially bridging ligands.

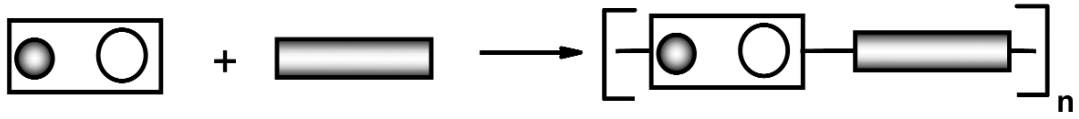

Scheme 2

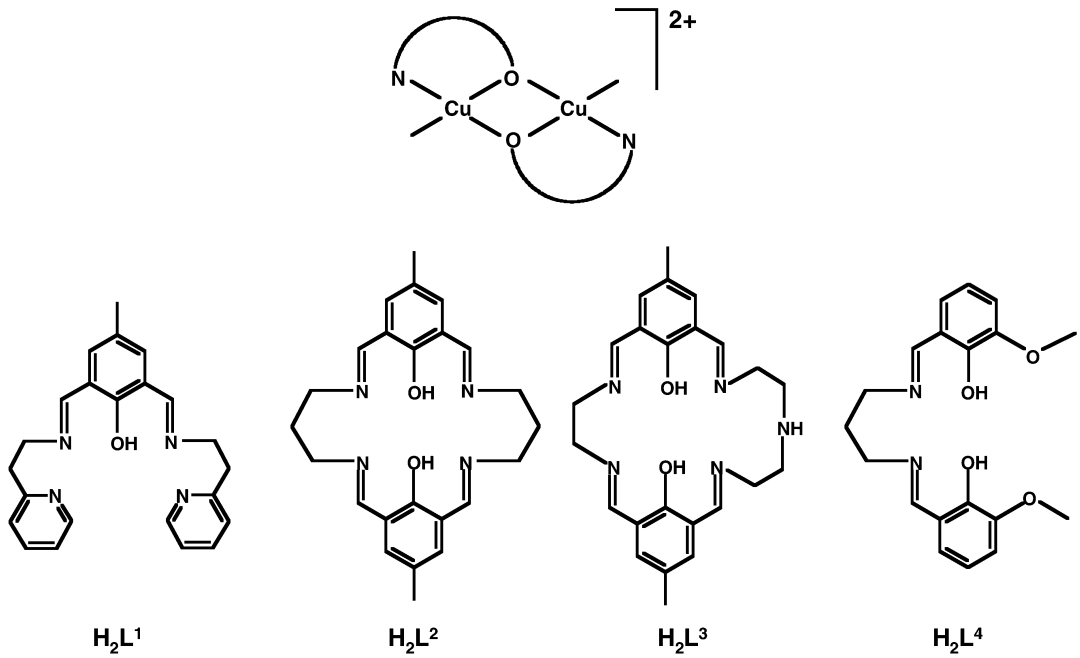

Scheme 3

This approach broadens the synthetic concept proposed by Cotton, Lin, and Murillo [6], which is based on binuclear metal–metal bonded cationic entities as building units.

ALKOXO-BRIDGED BINUCLEAR COPPER COMPLEXES AS NODES

A widely used strategy in designing coordination polymers is based upon the employment of divergent ligands, which connect metallic centers (the so-called "node-and-spacer" approach) [7]. The spacers can be either symmetrical or unsymmetrical bridging ligands.

The solid-state architecture (dimensionality, network topology) is determined by several factors: (i) metal-to-ligand stoichiometry; (ii) the stereochemical preference (coordination algorithm) of the assembling cations; (iii) the use of ancillary ligands attached to the metal ions or of additional bridging ligands; (iv) the intervention of the noncovalent interactions (hydrogen bonds, π–π stacking interactions); (v) the role of the anions (coordinated, bridging, uncoordinated); and (vi) the presence of the

organic guest molecules. The 1:1 ligand-to-metal ratio leads to either linear or zigzag chains [7]. By altering the stoichiometry, namely by increasing the ligand-to-metal ratio, 2D and 3D networks can be obtained. In this case, the structures are expanded either through supplementary metal-bridging ligand bonds, or through the convolution of coordinative, hydrogen-bonding, and π–π stacking interactions [8].

The reaction between a Cu(II) salt and amino alcohols affords, through the deprotonation of the OH group, alkoxo-bridged binuclear species, which can act as nodes in the construction of coordination polymers.

The following amino alcohols have been employed to generate binuclear alkoxo-bridged species: triethanolamine (H_3tea), diethanolamine (H_2dea), monoethanolamine (Hmea) and monopropanolamine (Hpa). As spacers, we used rigid bis(4-pyridyl) derivatives: 4,4'-bipyridyl (4,4'bpy) and bis(4-pyridyl)ethylene (bpe).

The amino alcohols with higher denticity (H_3tea, H_2dea) favor the formation of 1D coordination polymers. Conversely, in order to obtain coordination polymers with higher dimensionality, amino alcohols with lower denticity (Hmea, Hpa) have to be used (Scheme 4).

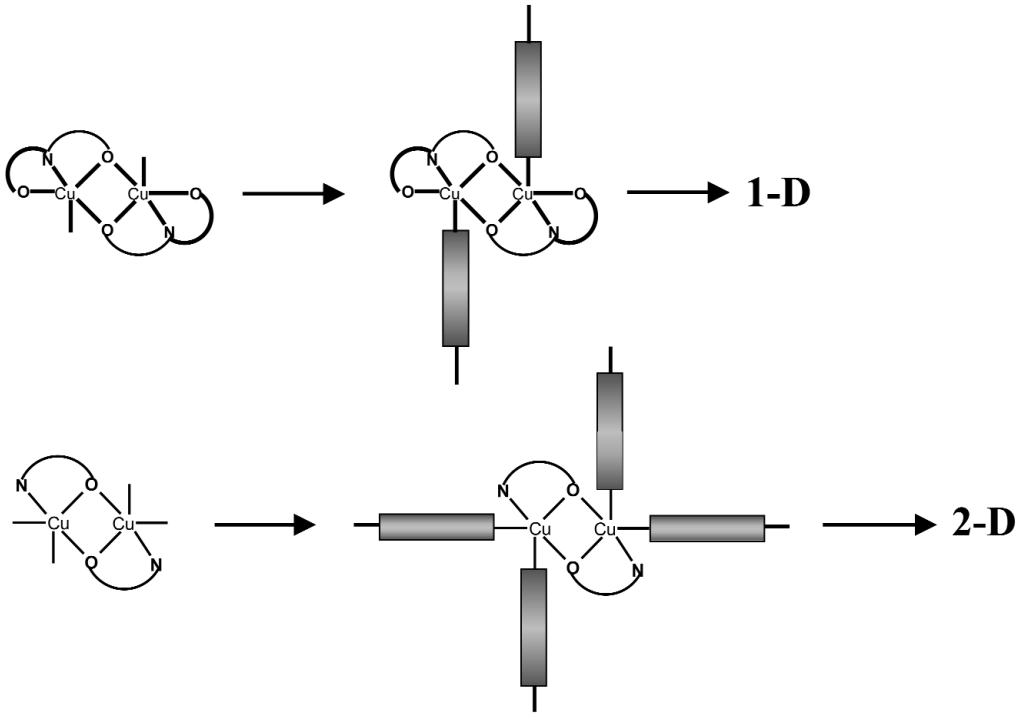

Scheme 4

ONE-DIMENSIONAL COORDINATION POLYMERS

The reactions between Cu(II) perchlorate, a divergent ligand, and H_3tea or H_2dea affords 1D coordination polymers: $[Cu_2(H_2tea)_2(bpe)](ClO_4)_2 \cdot (bpe) \cdot H_2O$ **1**, $[Cu_2(Hdea)_2(4,4'\text{-bipy})](ClO_4)_2$ **2**, $[Cu_2(Hdea)_2(bpe)] \cdot (bpe)(ClO_4)_2$ **3** (Fig. 1) [9,10].

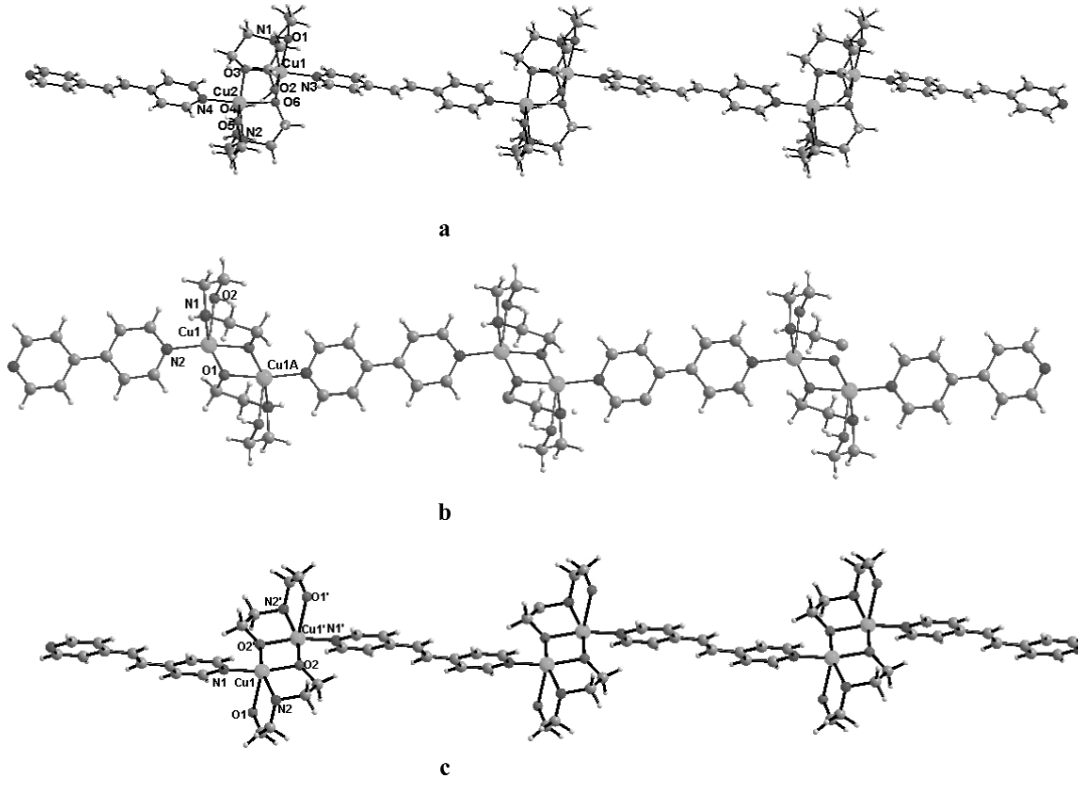

Fig. 1 Views of the 1D coordination polymers: $[Cu_2(H_2tea)_2(bpe)](ClO_4)_2 \cdot (bpe) \cdot H_2O$ **1**, $[Cu_2(Hdea)_2(4,4'\text{-bipy})](ClO_4)_2$ **2**, $[Cu_2(Hdea)_2(bpe)] \cdot (bpe)(ClO_4)_2$ **3**.

The presence of the uncoordinated bpe molecules in **1** and **3** leads to quite interesting supramolecular architectures. These molecules act as H-bond acceptors, connecting the 1D coordination polymers. In the case of **1**, the uncoordinated bpe molecules bind parallel chains, spread along the crystallographic *b* axis, through H-bonds, resulting in a double zigzag-ladder network (Fig. 2a). A channel is formed inside each ladder, which is occupied by perchlorate anions (Fig. 2b). Each $[Cu_2]$ node interacts with four bpe spacers: it forms coordination bonds with two bpe molecules, and H-bonds with the two others. The uncoordinated bpe molecules in **3** bind parallel chains through weak H-bond interactions established between the nitrogen atom and the C–H group from a bridging bpe molecule and between a C–H group and the oxygen atom from the coordinated OH group. Two-dimensional supramolecular layers with rhombic meshes are formed (Fig. 3).

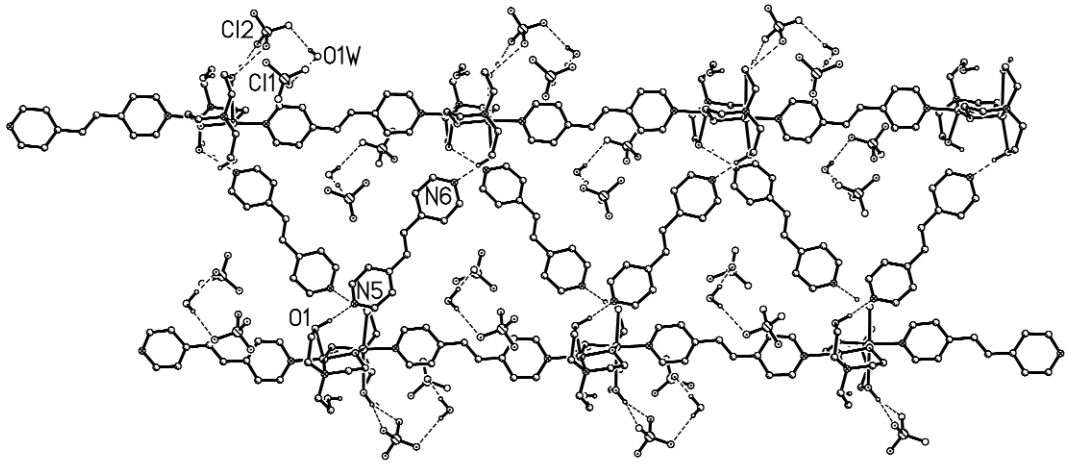

(a)

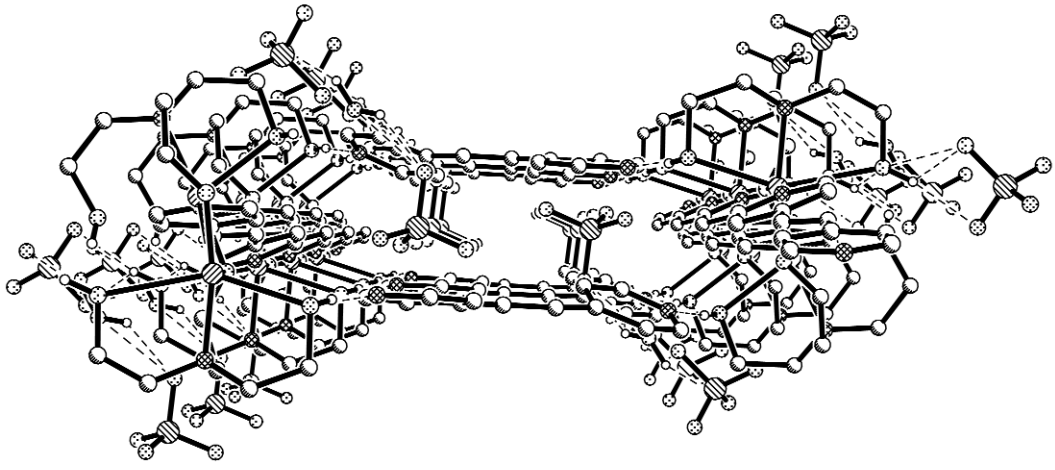

(b)

Fig. 2 Packing diagram of **1** illustrating the zigzag ladder architecture (a); view along the *b* axis, showing the formation of a channel inside the ladder (b).

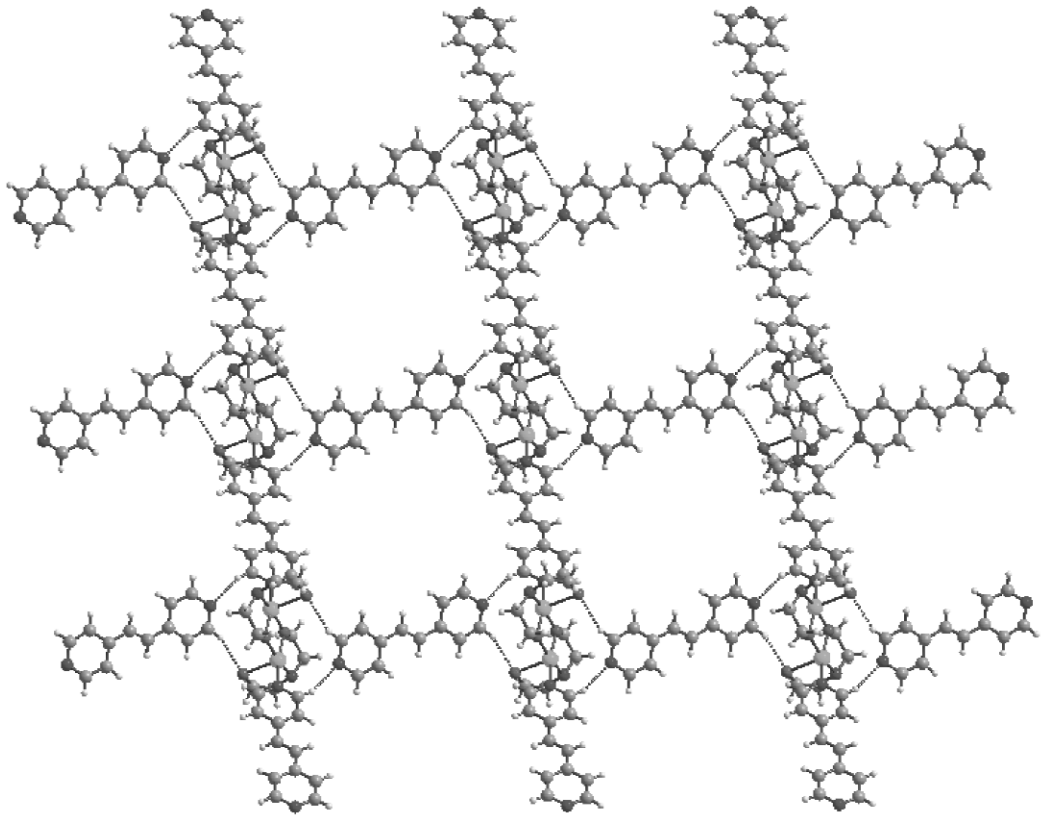

Fig. 3 Packing diagram of **3** showing the supramolecular grid-like architecture.

TWO-DIMENSIONAL COORDINATION POLYMERS

By employing bidentate amino alcohols, propanolamine, or monoethanolamine, 2D grid-like coordination polymers have been obtained: $[Cu_2(ap)_2(4,4'\text{-bipy})_2](ClO_4)_3 \cdot (4,4'\text{-bipy}) \cdot (H_2ap) \cdot (H_2O)$ **4**, and $[Cu_2(mea)_2(bpe)_2](ClO_4)_2$, **5** [9,10]. Figure 4 shows a fragment of the 2D network in **4**. The dimensions of the meshes are quite large: 12.31 × 13.36 Å in **4**, and 14.548 × 15.584 Å in **5**. Compounds **4** and **5** nicely illustrate how the problem of the empty space is solved. The 2D coordination networks in **4** stack parallel to one another, generating parallel channels running in the [1 0 –1] direction. These channels are marked in Fig. 5 through arrows. Each channel is filled by an interesting H-bonded polymer constructed from uncoordinated 4,4'-bipy and water molecules, H_2pa^+ (monoprotonated aminopropanol species) and perchlorate ions. On the other hand, compound **5** exhibits an interlocked 3D structure, resulting from the inclined interpenetration of 2D grid-like sheets. Each sheet is constructed from $[Cu_2(mea)_2]$ nodes, interconnected by bpe spacers. Every mesh of every sheet contains parts of two others passing through it (Fig. 6). The supramolecular architecture can be described as a 2D inclined catenation p–p (parallel–parallel) of (4,4) layers with Doc (2/2) [11].

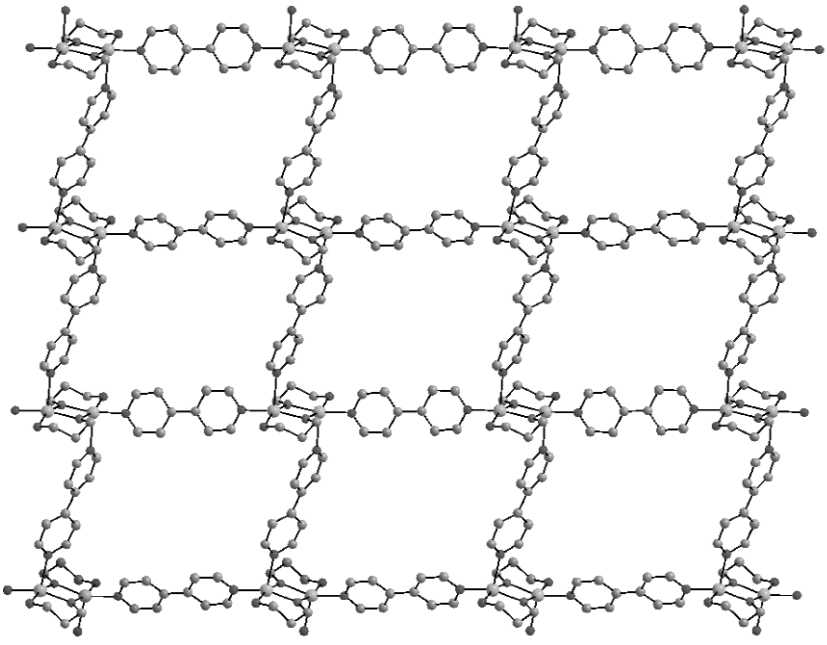

Fig. 4 View of the 2D coordination polymer $[Cu_2(ap)_2(4,4'\text{-bipy})_2](ClO_4)_3 \cdot (4,4'\text{-bipy}) \cdot (H_2ap) \cdot (H_2O)$ **4**.

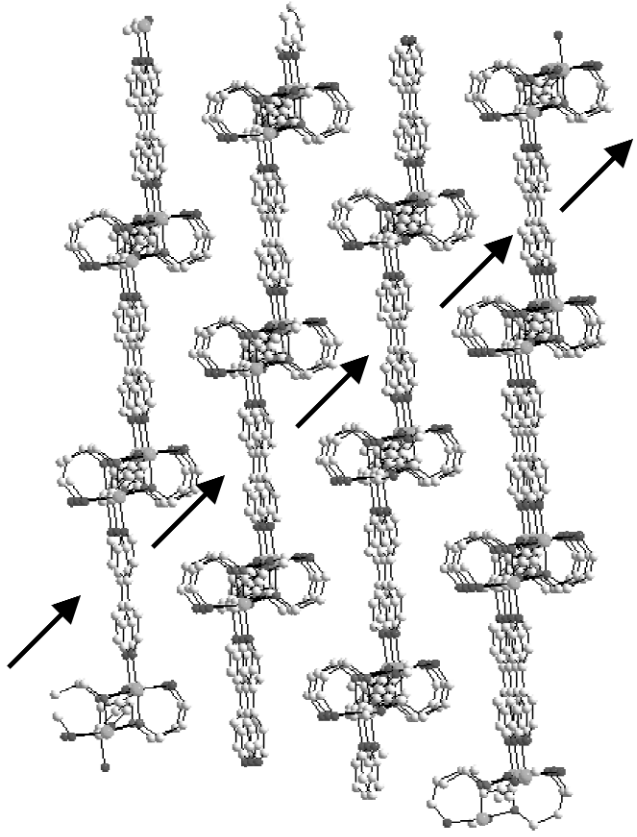

Fig. 5 Packing diagram showing the formation of the channels in compound **4**.

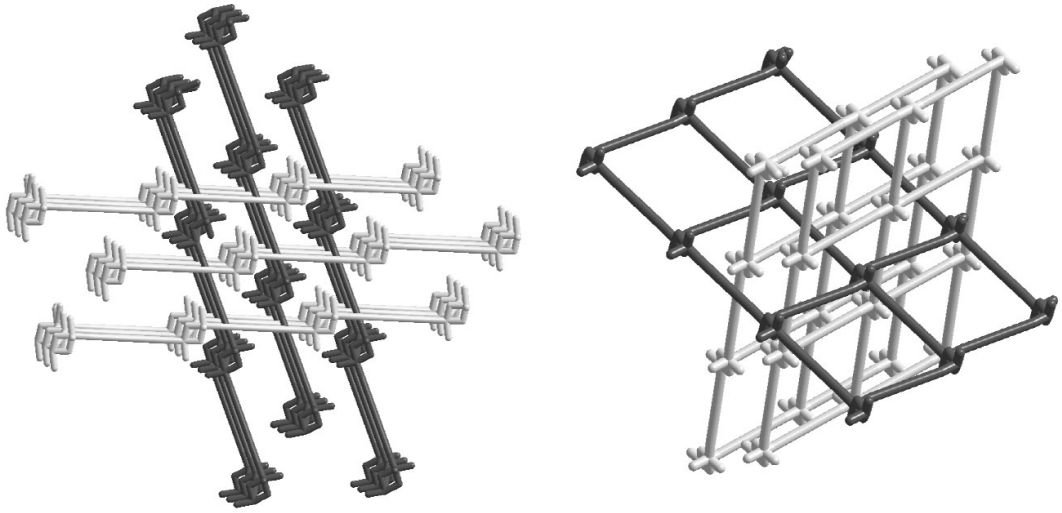

Fig. 6 Two views showing the inclined interpenetration mode of the 2D layers in **5**.

MOLECULAR RECTANGLES: TETRANUCLEAR COMPLEXES

The rational synthesis of multimetallic systems with pre-established nuclearities and topologies of the metallic centers, as well as with tunable distances between the metallic ions, is an important goal in modern coordination chemistry. All these characteristics are crucial for their magnetic or biomimetic properties. Three conditions must be fulfilled by a synthetic strategy leading to discrete polynuclear complexes: (i) control of the nuclearity, (ii) control of the topology of the metallic centers, and (iii) control of the distance between the metal ions. The latter condition is particularly important in the effort to mimic metallo-enzymes with both short (3–4 Å) and long (>10 Å) metal–metal separations, as, for example, in the case of multi-copper oxidases. The larger the number of metallic centers, the wider the variety of possible topologies. Taking the case of tetranuclear complexes, the metal ions can be displayed in several geometries: linear, tetrahedral, square, rectangular, butterfly, U-shaped, or heterocubane.

The molecular rectangles (two long and two short sides) can be obtained by combining the bridging ability of *exo*-dentate ligands, such as bis(4-pyridyl)derivatives, with the one of other ligands. For example, Hupp et al. [12], Sullivan et al. [13], and Lu et al. [14] have obtained molecular rectangles that are based on *fac*-$Re(CO)_3$ corners. Two edges are constructed from 4,4'-bipyridine molecules, while the other two are formed by *exo*-bidentate [pyrazine, bis(4-pyridyl)ethylene], or bis-chelating (2,2'-bipyrimidine), or alkoxo ligands.

An alternative way to design molecular rectangles consists in the use of binuclear Cu(II) complexes with compartmental end-off ligands [15–17]. Within the starting binuclear complexes, the Cu(II) ions frequently exhibit a coordination number of five and a square–pyramidal geometry. Our approach is based on the observation that the weakly coordinated ligands (e.g., perchlorato ions or solvent molecules), which are coordinated in the apical position to the metal ions, can be replaced by *exo*-dentate ligands, resulting in tetranuclear complexes (Scheme 5). As a compartmental ligand, we have used a classical one, namely 2,6-bis[*N*-(2-pyridylethyl)formimidoyl]4-methyl-phenolato (H_2L^1), which is a Schiff base obtained from the reaction of 2,6-diformyl-4-methyl-phenol with 2-(2-aminoethyl)pyridine. The starting binuclear complex contains the HO^- ion as an exogenous bridge. The distances between the metallic centers can be tuned by using appropriate spacers. The linkers are either symmetrical [e.g., bis(4-pyridyl)derivatives] or unsymmetrical ligands (e.g., the isonicotinatao anion). Figure 7 illustrates the crystal structures of four complexes obtained following this strategy:

$[\{L^1(\mu\text{-OH})Cu_2\}(\mu\text{-4,4'bipy})_2\{Cu_2(\mu\text{-OH})L^1\}](ClO_4)_4\cdot 3H_2O$**4**, **6**, $[\{L^1(\mu\text{-OH})Cu_2\}(\mu\text{-bpe})_2\{Cu_2(\mu\text{-OH})L^1\}](ClO_4)_4\cdot 4H_2O$**4** **7**, $[\{L^1(\mu\text{-OH})Cu_2\}(\mu\text{-bpeta})_2\{Cu_2(\mu\text{-OH})L^1\}](ClO_4)_4\cdot CH_3OH\cdot 1.5H_2O_4$ **8**, $[\{L^1(\mu\text{-OH})Cu_2\}(\mu\text{-IN})_2\{Cu_2(\mu\text{-OH})L^1\}](ClO_4)_2\cdot 2C_2H_5OH\cdot 0.5H_2O$ **9** [bpeta = bis(4-pyridyl)ethane]. In all these compounds, the Cu(II) ions exhibit a coordination number of five, with a square–pyramidal geometry, the basal plane being formed by two nitrogen atoms arising from the Schiff-base ligand, and two oxygen atoms (one from the phenolato endogenous bridge, and the other one from the hydroxo bridge). The apical positions are occupied by the nitrogen atoms from the *exo*-dentate ligands. The magnetic properties of the compounds belonging to this family are dominated by the strong antiferromagnetic interaction ($J = -300 \pm 30$ cm^{-1}) occurring between the Cu(II) ions residing on the short side of the rectangle.

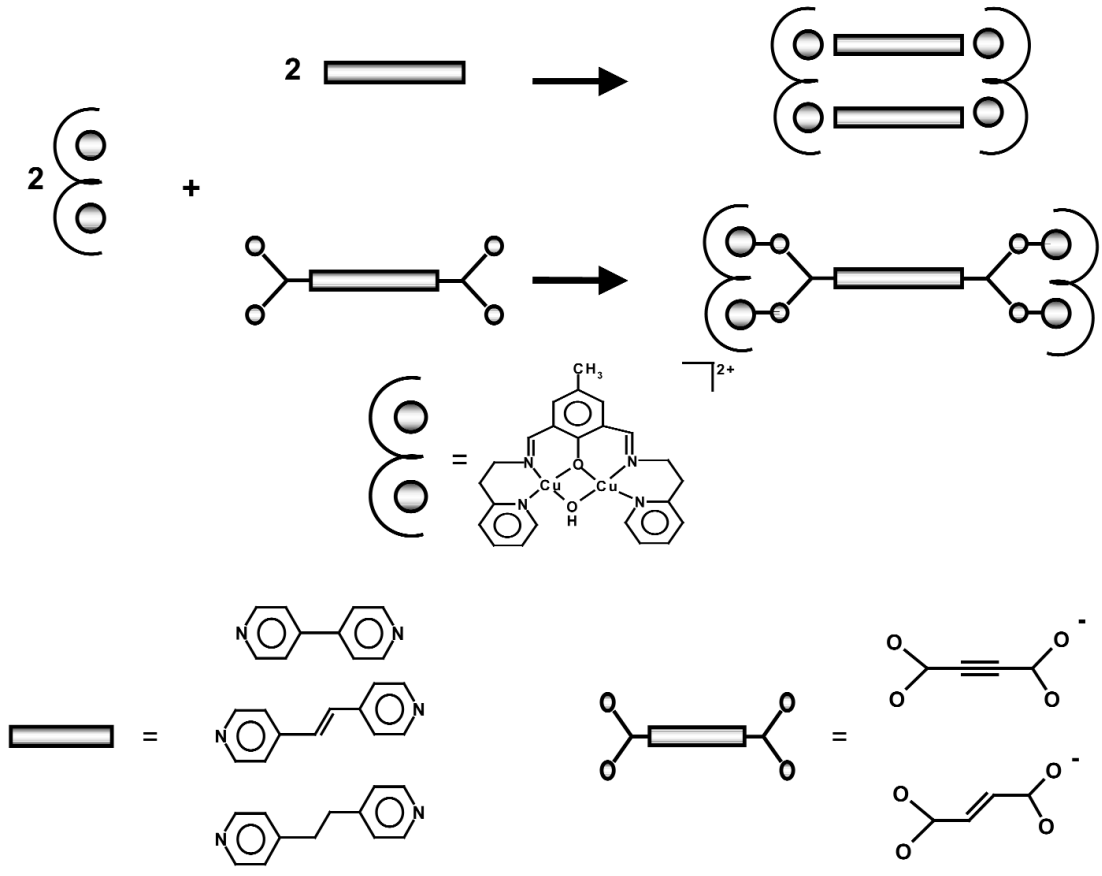

Scheme 5

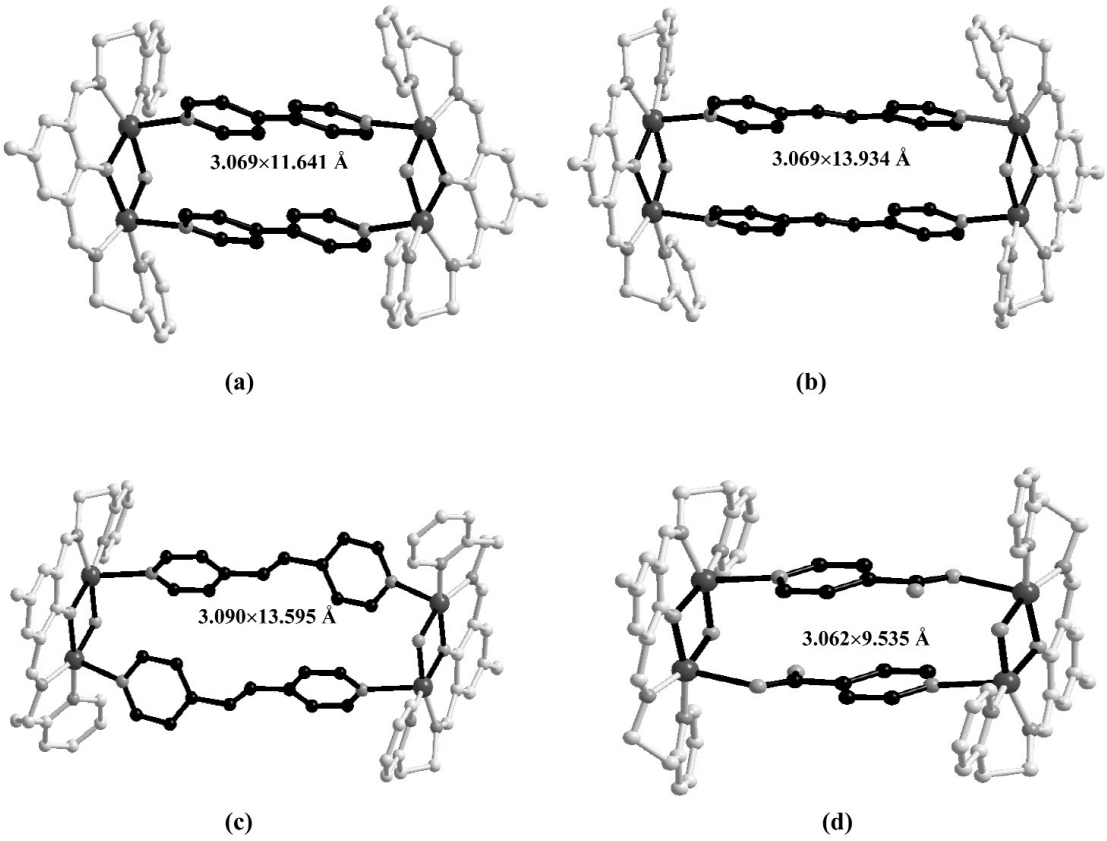

Fig. 7 Molecular rectangles obtained by self-assembly processes involving binuclear complexes and *exo*-dentate ligands: (a) 4,4'-bipyridine; (b) bis(4-pyridyl)ethylene; (c) bis(4-pyridyl)ethane [9]; (d) the isonicotinato ion.

It is worth noting that compounds **6**–**9** result also from a multicomponent self-assembly process, that is, the one-pot reaction between the Schiff-base, exo-dentate ligand, lithium hydroxide, and Cu(II)perchlorate.

A similar tetra-zinc rectangle, isostructural with **7**, has been characterized recently: the two binuclear entities, $[L^1(\mu\text{-OH})Zn_2]^{2+}$, are connected through two *trans*-1,2-bis(4-pyridyl)ethylene molecules. It exhibits a very interesting single-crystal-to-single-crystal photoreaction of the bis(4-pyridyl)ethylene ligands, to give tetrakis(4-pyridyl)cyclobutane [18].

We have also shown that this synthetic approach, "dimer-of-dimers", can be extended by using bis(bidentate) ligands, such as the anions of dicarboxylic acids (e.g., acetylenedicarboxylic acid, fumaric acid). The dicarboxylato ligand links two bimetallic moieties resulting in tetranuclear complexes with the metallic ions located in the corners of a rectangle: $[\{L^1(\mu\text{-OH})Cu_2\}(\mu\text{-acdca})\{Cu_2(\mu\text{-OH})L^1\}](ClO_4)_2$ **10**, $[\{L^1(\mu\text{-OH})Cu_2\}(\mu\text{-fum})\{Cu_2(\mu\text{-OH})L^1\}](ClO_4)_2$ **11** (Fig. 8) [16,17]. Each carboxylato group forms a third bridge between the Cu ions within the binuclear moiety (*syn–syn* bridging mode). The stereochemistry of the Cu(II) ions is square–pyramidal.

When the compartmental ligand is a macrocyclic one, for example, the Schiff base resulted from the condensation of 2,6-diformyl-4-methyl-phenol with 1,3-diamino-propane (H_2L^2), the reaction with a linear dicarboxylato anion (e.g., acetylenedicarboxylato, $acdca^{2-}$) leads to a 1D coordination polymer $[Cu_2L^2(acdca)]\cdot CH_3OH\cdot 4H_2O$ **12** (Fig. 9) [19] The Cu(II) ions exhibit an elongated octahedral geometry.

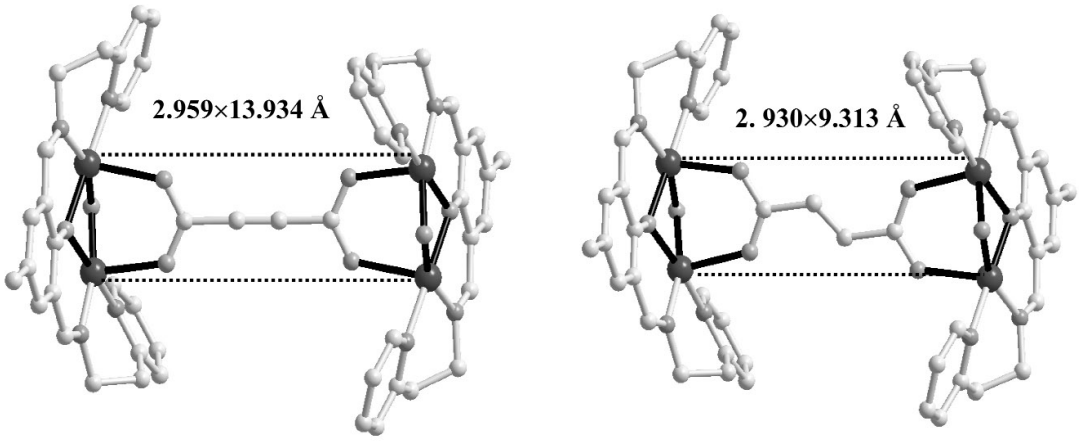

Fig. 8 Tetranuclear complexes obtained by self-assembly processes involving binuclear complexes and *exo*-dentate ligands: (a) acetynenedicarboxylato; (b) fumarato.

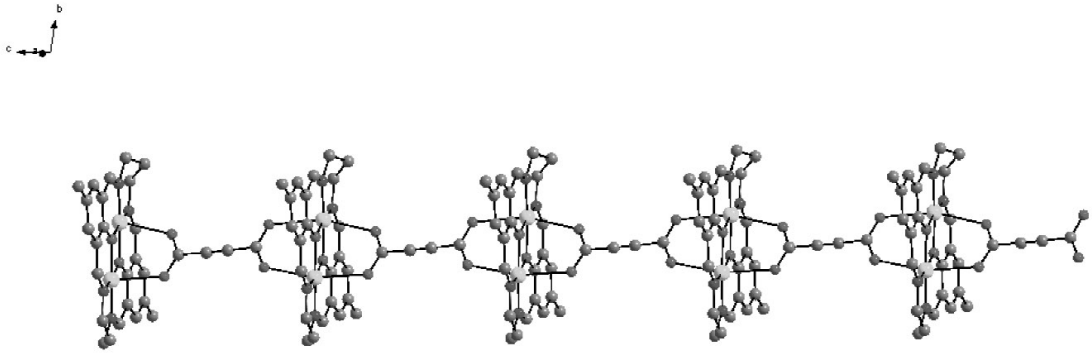

Fig. 9 View of the polymeric chain $_{\infty}^{1}[Cu_2L^2(acdca)]$,·**12**.

HETEROMETALLIC COMPLEXES

3d-3d' Heterobimetallics

Binuclear complexes with different metal ions are particularly attractive as building blocks in designing heterometallic complexes. They combine the electronic and stereochemical peculiarities of two metal ions. For example, the reaction between a [CuZn] complex and bis(4-pyridyl)ethylene afforded a heterometallic molecular rectangle $[(CuZnL^3)_2(bpete)_2](ClO_4)_4 \cdot 4.5 \cdot CH_3OH$ **13**, Fig. 10 [H_2L^3 is a dissymmetric macrocyclic Robson proligand that resulted from 2,6-diformyl-4-methyl-phenol, ethylenediamine, and diethylenetriamine (Scheme 3)] [19]. The Cu(II) ions are pentacoordinated with a square planar geometry, in which the apical position is occupied by the nitrogen atom arising from the bpete linker [Cu(1)–N(6) = 2.297(6) Å]. The basal plane is formed by two nitrogen atoms arising from the Schiff-base ligand, and two phenoxo oxygen atoms, with the Cu–O and Cu–N distances falling in the range 1.919(5)–1.949(5) Å. The zinc ions are coordinated by two imino nitrogen atoms arising from the Schiff-base [Zn(1)–N(4) = 2.080(9) Å; Zn(1)–N(2) = 2.032(7) Å], two phenoxo oxygens [Zn(1)–O(1) = 2.220(5) Å; Zn(1)–O(2) = 2.168(5) Å] and one nitrogen atom from the bpete bridge [Zn(1)–N(7) = 2.059(6) Å]. The secondary amine nitrogen, N(5), can be considered as being semi-coordinated

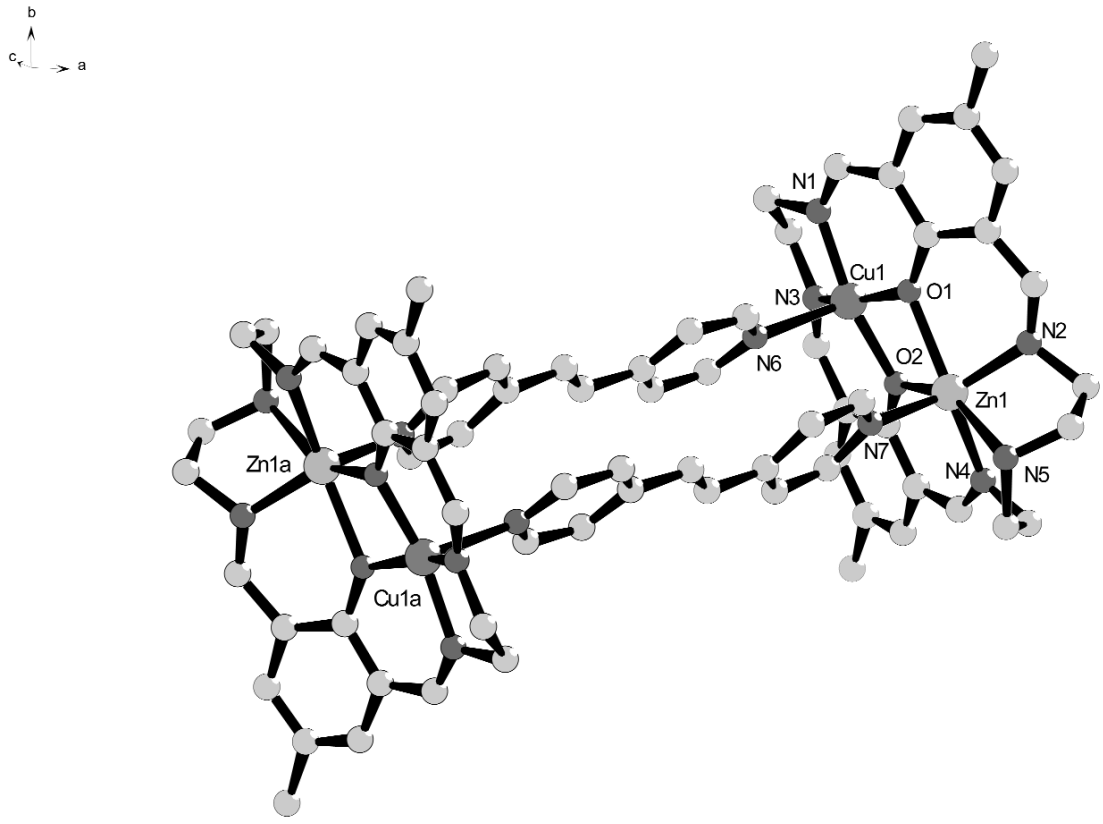

Fig. 10 Perspective view of the $[Cu_2Zn_2]$ molecular rectangle, **13**.

[Zn(1)–N(5) = 2.650(2) Å]. The distances between the diagonally disposed metal ions are: Cu(1)···Cu(1a) = 13.84 Å, and Zn(1)···Zn(1a) = 14.28 Å. The room-temperature value of the $\chi_M T$ product (χ_M is the paramagnetic susceptibility) is in line with the presence of two isolated, uncoupled Cu(II) ions: 0.90 $cm^3\ mol^{-1}\ K$ (the calculated value, assuming $g = 2.2$, is 0.91 $cm^3\ mol^{-1}\ K$).

More exciting from the magnetic point of view are binuclear species with two different paramagnetic ions. The self-assembly process between $[MnCuL^3]^{2+}$ cations and the trimesate ion leads to a hexanuclear complex with the formula $[\{MnCuL^3\}_3(tma)](ClO_4)_3 \cdot 8H_2O$ **14** [20]. Three [MnCu] entities are connected through the tma^{3-} anion, resulting in a complex entity with a C_3 symmetry axis (Fig. 11). The Mn(II) and Cu(II) ions within each pair are bridged by two phenoxo oxygen atoms and by a carboxylato group (*syn–syn* bridging mode) arising from the tma^{3-} spacer. The three short Mn···Cu distances are 3.109(2) Å. The intramolecular Mn···Mn and Cu···Cu distances are, respectively, 9.847 and 10.179 Å.

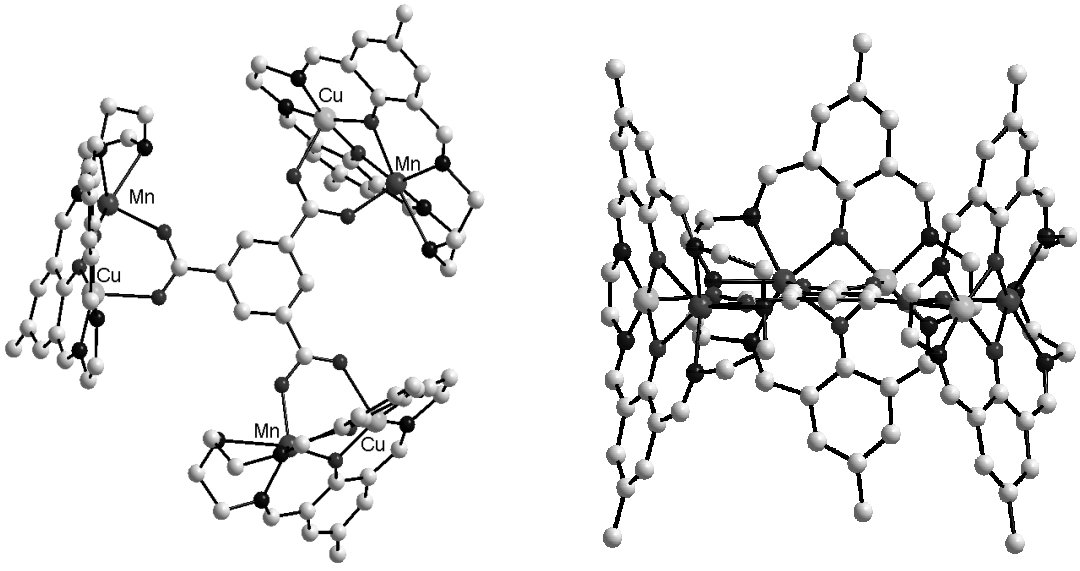

Fig. 11 Perspective views of the hexanuclear cation in **14**: (a) top view; (b) side view.

This trimesate anion has been chosen as a bridge not only because of its potential ability to bridge 3×2 metal ions, but also since it fulfils the necessary conditions to mediate a ferromagnetic coupling through a spin polarization mechanism [21]: the whole bridging molecule can be planar, and the metallic centers are separated by an odd number of atoms. Indeed, the magnetic properties of this compound are quite interesting. The $\chi_M T$ vs. T plot is given in Fig. 12. At room temperature, the value of the $\chi_M T$ product is 13.5 $cm^3\ mol^{-1}\ K$, which roughly corresponds to six uncoupled metal ions, $3Mn^{2+}$ and $3Cu^{2+}$ (the calculated value is 14.2 $cm^3\ mol^{-1}\ K$). By decreasing the temperature, $\chi_M T$ decreases more and more, reaching a minimum (8.8 $cm^3\ mol^{-1}\ K$) at 12 K. Below 12 K, the $\chi_M T$ product increases abruptly. This behavior can be explained as follows: the exchange interaction within each Mn(II)–Cu(II) pair is supposed to be much stronger than the exchange interaction between the metal ions belonging to different pairs. The magnetic behavior of **14** between room temperature and slightly above 12 K can be described considering only three magnetically isolated Cu^{II}–Mn^{II} binuclear units with $J_1 = -16.7\ cm^{-1}$ (see dashed line in Fig. 12). The minimum around 12 K corresponds to three uncorrelated $S = 2$ spins. At $T < 12$ K, the ferromagnetic coupling among the resulting three $S = 2$ spin units through the spin polarization mechanism (Scheme 6) causes the observed increase of $\chi_M T$. The value of the exchange coupling constant involving the three $S = 2$ spins is $J_{eff} = +0.05\ cm^{-1}$.

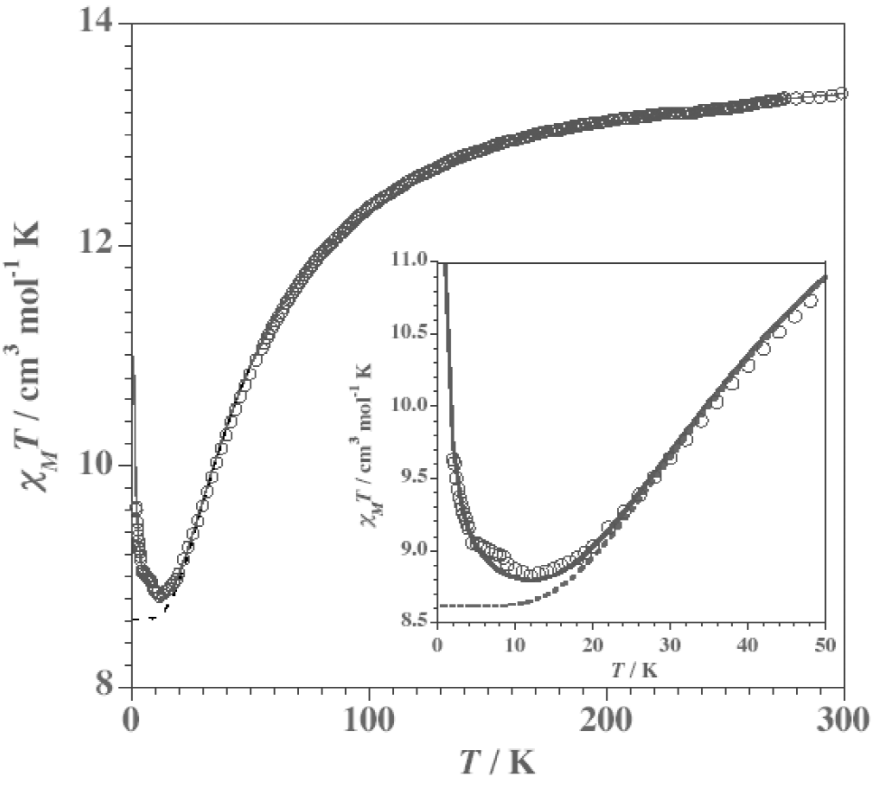

Fig. 12 $\chi_M T$ vs. T plot for compound **14**: (o) experimental data; (——) best-fit curve; (-----) best-fit curve considering three magnetically isolated Cu^{II}–Mn^{II} pairs. The insert shows a detail of the low-temperature region.

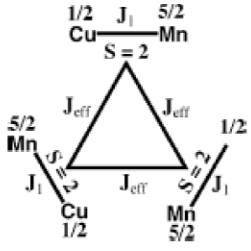

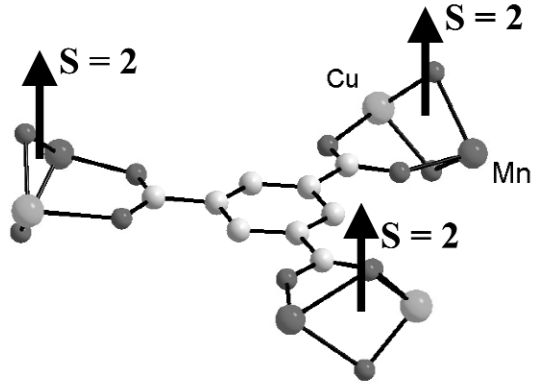

Scheme 6

3d-4f Heterobimetallics

The versatility of the heterometallic binuclear building blocks increases when the two metal ions differ drastically through their chemical behavior, since the metal ions can interact selectively with various spacers. This is the case of the 3d-4f heterobinuclear complexes: the rare-earth cations are hard acids and exhibit high coordination numbers, whereas Cu(II) is a borderline acid with a marked tendency to adopt a more or less distorted square–pyramidal geometry. From this perspective, the use of the isonicotinato anion (IN^-), as an unsymmetrical linker, is very appealing: the rare-earth cations are extremely oxophilic and will, therefore, prefer to interact with the carboxylato group, while the Cu(II) ion will bind to the nitrogen atom of the pyridyl group.

As building blocks, we employ heterobinuclear 3d-4f species with side-off compartmental Schiff-base ligands: $[Cu^{II}Ln^{III}L^4(NO_3)_3]$ (H_2L^4 = the Schiff base obtained from the 2:1 condensation of 3-methoxysalyciladehyde with 1,3-propanediamine, Scheme 3) [22].

By reacting $[CuPrL^4(NO_3)_3]$ with lithium isonicotinate, we obtained a compound with the formula $[CuPrL^4(NO_3)_2(IN)]$ **15**, whose crystal structure is in line with our expectations [23]. Indeed, the binuclear [CuPr] units are connected by the isonicotinato ligand, which is coordinated through the carboxylato group to two Pr(III) ions and with the nitrogen atom to the Cu(II) ion. So each IN^- is coordinated simultaneously to three metallic centers: two Pr(III) and one Cu(II). Two Pr(III) ions arising from two $\{CuPrL^4\}$ units are bridged by two carboxylato groups from two isonicotinato bridges (*syn–syn* bridging mode). The Pr···Cu distance within the [PrCu] building block is 3.611(1) Å. The extension of the structure can be described as follows: two praseodymium ions are bridged by two carboxylato groups, resulting in rhomboidal $\{Pr_2(O_2C)_2\}$ rings. These rings are interconnected through the pyridyl moieties of the isonicotinato bridges, which coordinate to the Cu(II) ions. Large polygons containing four Pr(III) and four Cu(II) ions are formed (Scheme 7). Each [CuPr] unit is connected through three isonicotinato bridges to five other [CuPr] units, resulting in 2D layers (Fig. 13). The distances between the Cu atom and the two praseodymium atoms bridged by the same IN^- ion are slightly different: 8.75 and 9.30 Å. The room-temperature value of the $\chi_M T$ product is 2.11 $cm^3\ mol^{-1}$ K, which corresponds to the expected one, calculated using the equation $\chi_M T = (Ng_{Cu}{}^2\beta^2/3k)[S_{Cu}(S_{Cu} + 1)] + (Ng_{Pr}{}^2\beta^2/3k)[J_{Pr}(J_{Pr} + 1)]$.

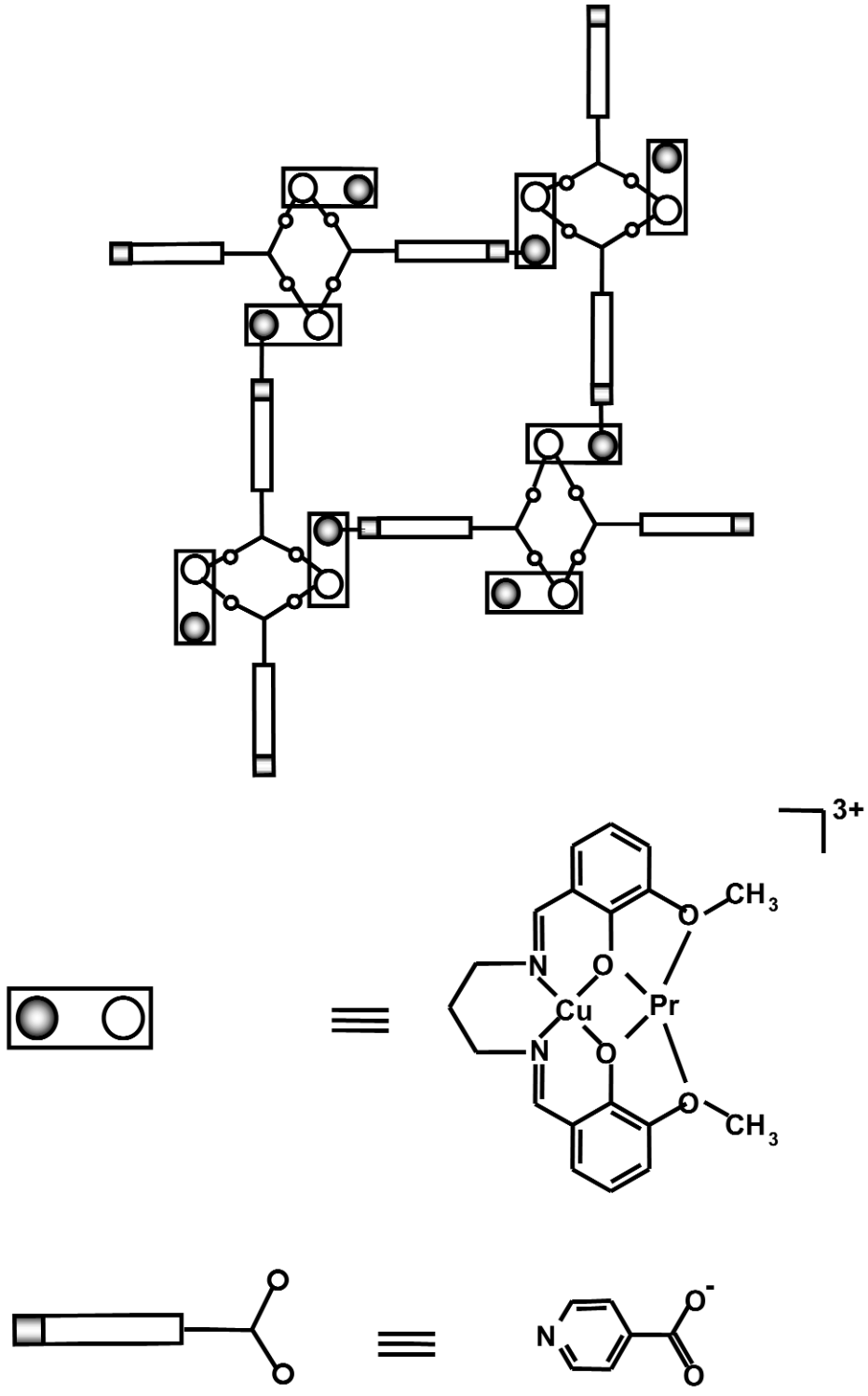

Scheme 7

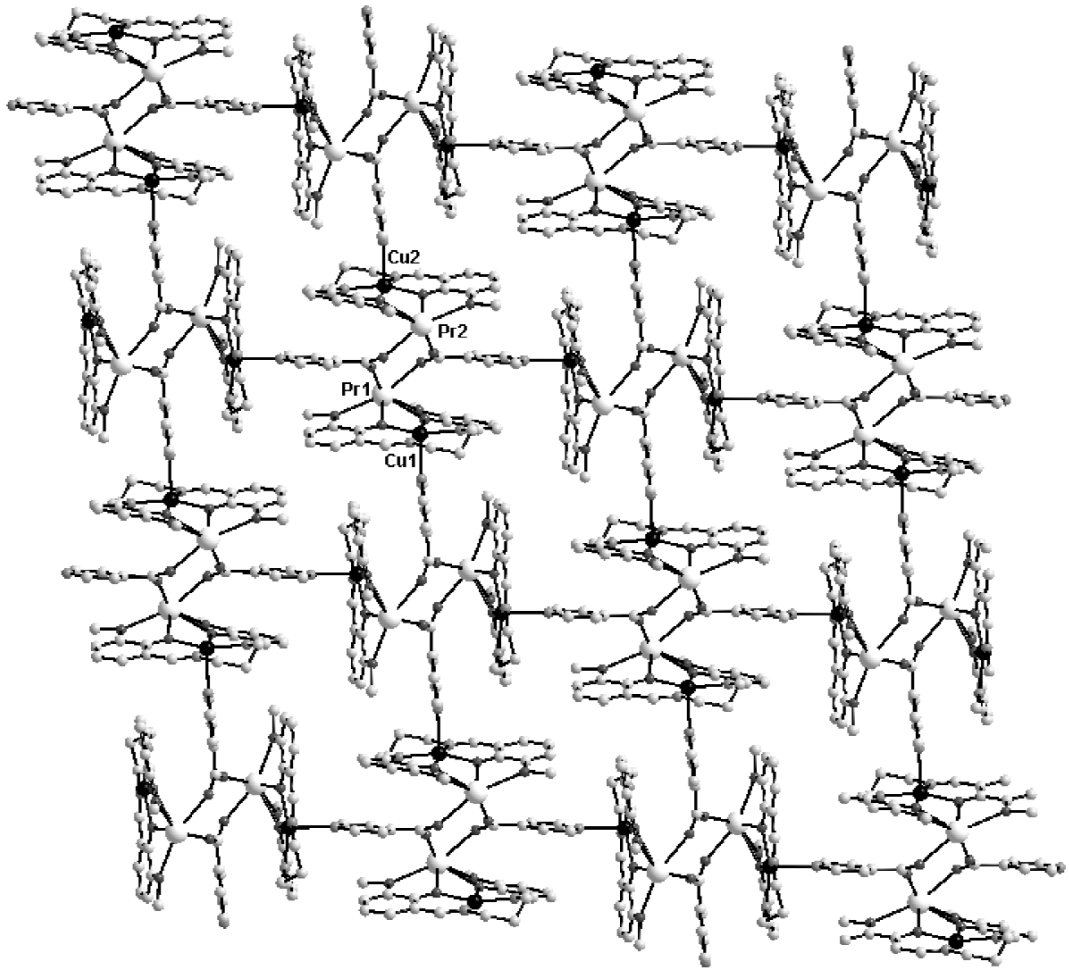

Fig. 13 View of the 2D network in **15**. For the sake of clarity, the nitrato groups coordinated to Pr have been omitted.

TOWARD COMPLEXES WITH THREE DIFFERENT SPIN CARRIERS

The synthetic approach based upon 3d-4f building blocks was further extended toward the construction of coordination polymers containing three different spin carriers: 3d-3d'-4f and 2p-3d-4f systems. Such compounds are of high interest in molecular magnetism, providing both physicists and theoreticians exciting cases for investigation.

The reaction between $[CuLnL^4(NO_3)_3]$ and $K_3Fe(CN)_6]$ (Scheme 8) led to a novel heterospin system, $[\{CuL^4\}Gd(H_2O)_3\{Fe(CN)_6\}]\cdot 4H_2O$ **16**, whose crystal structure has been solved [24]. This represents a straightforward synthetic route toward 3d-3d'-4f systems, by using heteronuclear 3d-4f cationic species as building blocks, and anionic complexes bearing the third paramagnetic ion, as linkers. The [CuGd] moiety preserves the structural features of the whole $[Cu^{II}Ln^{III}]$ family of complexes with compartmental Schiff-base ligands derived from 3-methoxysalicylaldimine: The Cu(II) ion is hosted in the inner N_2O_2 compartment, and the oxophilic gadolinium ion occupies the outer O_4 cavity (two oxygen atoms arise from the bridging phenoxo groups, two others from the methoxy ones). The Cu···Gd distance is 3.509(1) Å. The $[Fe(CN)_6]^{3-}$ ion connects three metal ions, through three meridially disposed cyano groups, resulting in a unique ladder-type topology (Fig. 14).

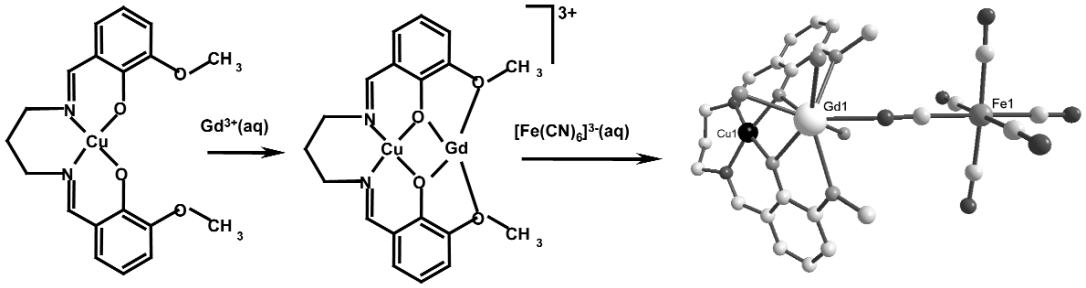

Scheme 8

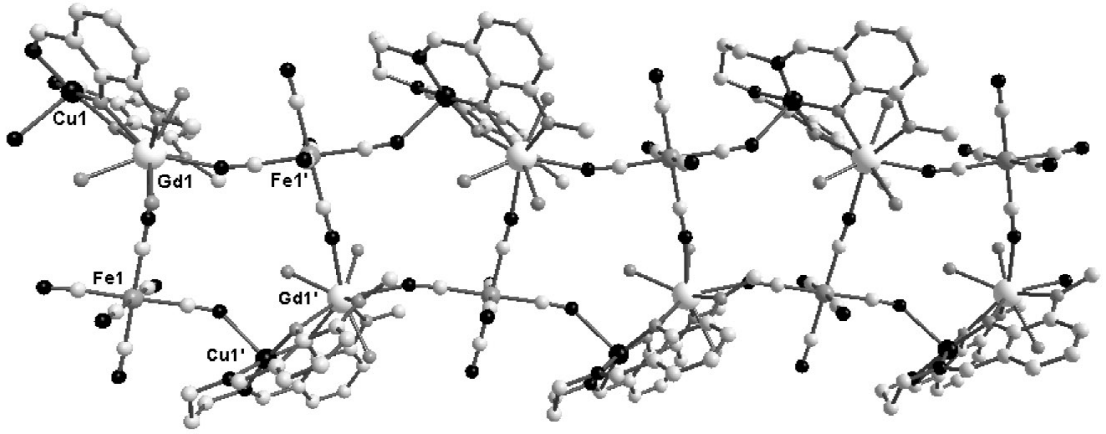

Fig. 14 Perspective view of a ladder chain in **16**.

The most intriguing properties of a heterospin system, such as **16**, are the magnetic ones. Magnetic susceptibility data for **16** were collected in the temperature range 1.9–300 K (Fig. 15). The value of the $\chi_M T$ product at room temperature is 9.04 cm^3 mol^{-1} K, which is higher than the calculated one (8.62 cm^3 mol^{-1} K) corresponding to the sum of the contributions of the three uncoupled ions, $(\chi_M T)_{HT} = (Ng^2\beta^2/3k)[S_{Gd}(S_{Gd} + 1) + S_{Cu}(S_{Cu} + 1) + S_{Fe}(S_{Fe} + 1)]$, with $g_{Cu} = g_{Gd} = g_{Fe} = 2$. The first-order orbital momentum associated to the low-spin Fe(III) ion is responsible for this difference. Upon lowering the temperature, $\chi_M T$ remains constant down to about 95 K, then increases and reaches a maximum (10.05 cm^3 mol^{-1} K) at 13.8 K. Below this temperature, $\chi_M T$ decreases abruptly (7.25 cm^3 mol^{-1} K at 1.9 K). The complex topology of the spin carriers in **16** makes the interpretation of its magnetic properties difficult. Additional information is obtained by analyzing the magnetic properties of the isostructural [CuGdCo] compound **17**, where Fe(III) ions are replaced by diamagnetic Co(III) ones. The temperature dependence of the $\chi_M T$ product for **17** exhibits the well-known characteristic feature of the [CuGd] binuclear units, namely, a ferromagnetic interaction of the two metal ions. Moreover, this ferromagnetic interaction is further supported by the field dependence of the magnetization, which shows an $S = 4$ ground state. No decrease of $\chi_M T$ at low temperatures is observed. This indicates that no antiferromagnetic interaction occurs between the [CuGd] units within the chain. The best fit to the data leads to the following parameters: $J_{CuGd} = 7.24$ cm^{-1}, $g_{av} = 2.00$ ($\boldsymbol{H} = -J\boldsymbol{S}_{Cu}\boldsymbol{S}_{Gd}$). Let us come back to compound **16**. First of all, we notice that the difference between the room-temperature value of its $\chi_M T$ product and the one of the Co(III) derivative, $\chi_M T(\mathbf{16}) - \chi_M T(\mathbf{17}) = 0.61$ cm^3 mol^{-1} K, represents the contribution of Fe(III). This value is close to those found for Fe(III) in several bimetallic [Gd(III)Fe(III)] compounds [25]. The [CuGd] units are connected through paramagnetic $[Fe(CN)_6]^{3-}$ building blocks, each one coordinating simultaneously to Cu(II) and Gd(III) ions. Since

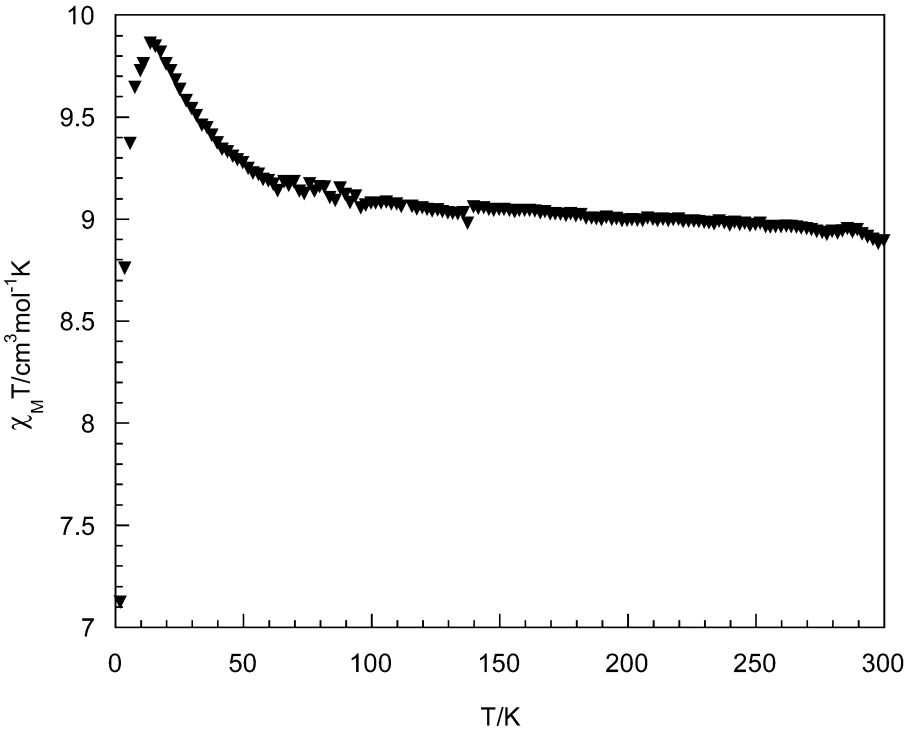

Fig. 15 $\chi_M T$ vs. T plot for compound **16**.

one CN group is coordinated to the axial position of the square pyramidal Cu(II), its magnetic orbital, d_{x2-y2}, being localized in the basal plane, one may assume that no magnetic interaction occurs between Cu(II) and Fe(III). On the other hand, the Gd(III)-NC-Fe(III) pathway is effective, as shown with several [Gd(III)Fe(III)] cyano-bridged systems which have been recently investigated [12]. Very weak ferro- and antiferromagnetic interactions were found ($|J| < 1$ cm^{-1}). A tentative interpretation of the magnetic behavior of **16** is as follows: Below 14 K, the Cu(II) and Gd(III) ions are ferromagnetically coupled, resulting in units with $S = 4$, as in the isostructural compound **17**. These units further interact antiferromagnetically with the paramagnetic $[Fe(CN)_6]^{3-}$ linkers. This explains the decrease of the $\chi_M T$ product bellow 14 K. According to the literature data [25], the Gd(III)–NC–Fe(III) interaction is supposed to be much weaker than the Cu(II) –Gd(III) one. Theoretically, a ferrimagnetic chain [($S = 4$) – ($S = -1/2$) – ($S = 4$) – ($S = -1/2$) –⋯] may result. The [$Cu^{II}Gd^{III}Cr^{III}$] complex is isomorphous with compounds **16** and **17**.

The reaction between the mononuclear precursor, [CuL^4] with gadolinium nitrate and LiTCNQ affords a unique compound, with three different spin carriers: 2p($TCNQ^{\bullet-}$)-3d(Cu^{2+})-4f(Gd^{3+}): [{CuL^4}$_2$Gd(TCNQ)$_2$]·(TCNQ)·(CH_3OH)·2CH_3CN, **18** [26]. The structure of **18** can be described as being constructed from almost linear trinuclear [Cu_2Gd] units on which the $TCNQ^{\bullet-}$ anionic radicals are attached (Fig. 16). The $TCNQ^{\bullet-}$ ions are further involved in both stacking and weak coordinative interactions, leading to a unique supramolecular architecture (Fig. 17). The three $TCNQ^{\bullet-}$ anions corresponding to a [Cu_2Gd] triad are parallel and aligned with their longitudinal axis along the *b* direction. The small separations between the **A**-**B**, and **B**-**C** anionic radicals (3.12 and, respectively, 3.32 Å) indicate the occurrence of the π–π interactions. Each **C**-$TCNQ^{\bullet-}$ radical interacts further with another uncoordinated radical, **C'**, the separation between them being 3.19 Å. Consequently, the overlap of the $TCNQ^{\bullet-}$ π clouds generate **ABCC'B'A'** stacks which connect pairs of $[Cu_2Gd(TCNQ)_2]_n^{n+}$ chains. The stacking interactions between $TCNQ^{\bullet-}$ radicals lead to diamagnetic $(TCNQ)_2^{2-}$ dimers.

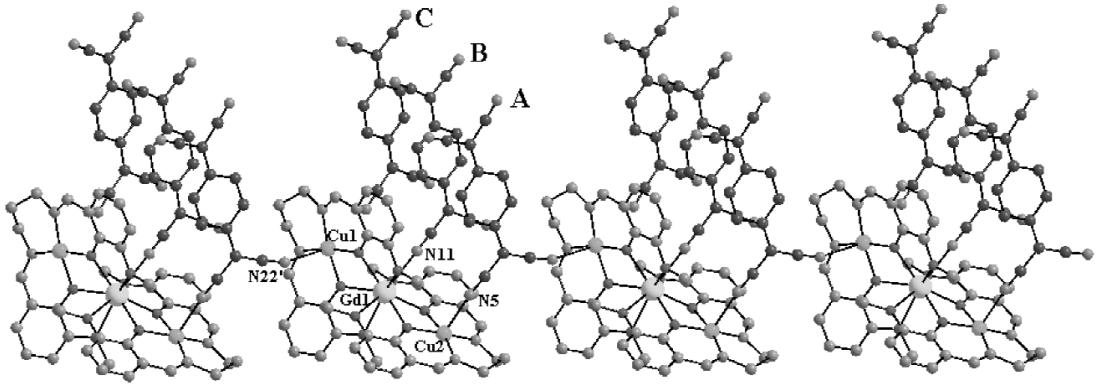

Fig. 16 View of a coordination polymer in **18**.

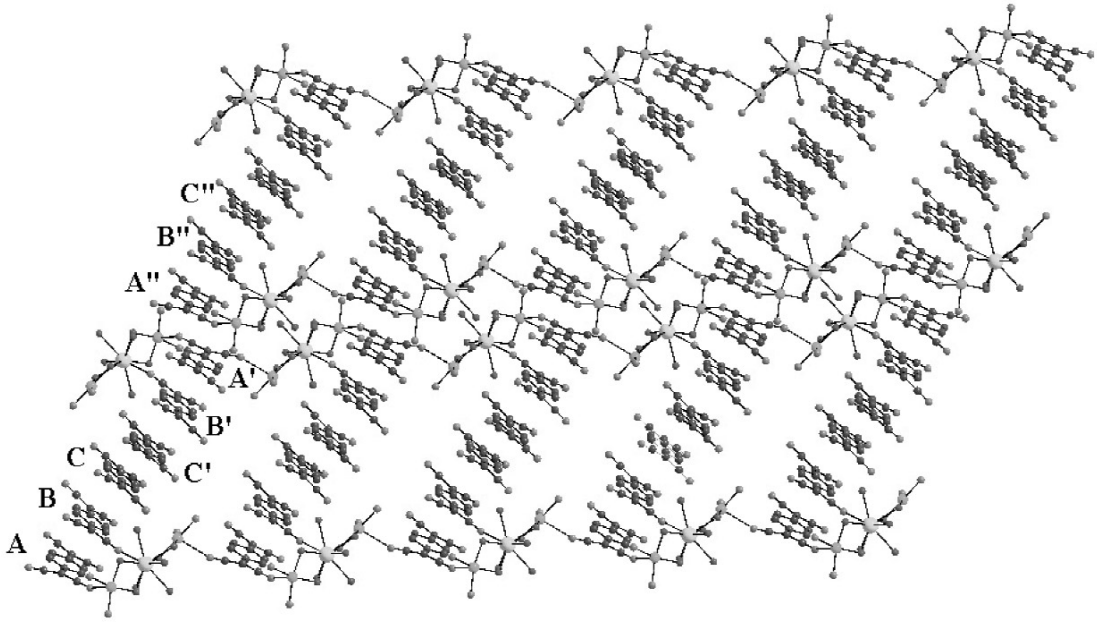

Fig. 17 Packing diagram for compound **18** (for the sake of clarity, the carbon atoms from the compartmental ligands have been removed).

Considering that the $TCNQ^{\bullet-}$ ions do not contribute to the magnetic moment of **1**, the magnetic properties can be interpreted by taking into account only the isolated [Cu_2Gd] triads. Indeed, the high-temperature limit of the $\chi_M T$ product corresponds to a magnetically noninteracting Cu(II)–Gd(III)–Cu(II) (1/2-7/2-1/2) system. As the temperature is lowered, $\chi_M T$ increases reaching a maximum at 10 K with $\chi_M T$ = 13.0 cm^3 mol^{-1} K. This behavior indicates that the Gd(III)–Cu(II) interaction is ferromagnetic with a ground state S = 9/2.

CONCLUSIONS AND OUTLOOK

The synthetic approach described herein opens interesting perspectives in crystal engineering, as well as in molecular magnetism. Novel solid-state architectures can be constructed by using binuclear nodes instead of monometallic ones. This chemistry can be further developed by using other organic molecule

as spacers, or metal-containing anions which can act as ligands. The intra-node exchange interaction combined with the one arising from the inter-node interactions could lead to materials with exciting magnetic properties. Moreover, the rational design of coordination polymers containing three different spin carries is of interest in the effort to obtain single-chain magnets.

ACKNOWLEDGMENTS

I would like to express my gratitude to all my coworkers, colleagues, and students. Their names appear in the references listed.

REFERENCES

1. (a) O. Kahn. *Adv. Inorg. Chem.* **43**, 179–259 (1995); (b) O. Kahn. *Acc. Chem. Res.* **33**, 647–657 (2000); (c) M. Eddaoudi, D. B. Moler, H. Li, B. Chen, T. M. Reinecke, M. O'Keeffe, O. M. Yaghi. *Acc. Chem. Res.* **34**, 319 (2001).
2. R. Ruiz, J. Faus, F. Lloret, M. Julve, Y. Journaux. *Coord. Chem. Rev*. **193–195**, 1069 (1999).
3. See, for example: (a) J. Černák, M. Orendáč, I. Potočňák, J. Chomič, A. Orendáčová, J. Skoršepa, A. Feher. *Coord. Chem. Rev.* **224**, 51 (2002); (b) M. Ohba and H. Okawa. *Coord. Chem. Rev.* **198**, 313 (2000); (c) K. R. Dunbar and R. A. Heintz. *Progr. Inorg. Chem*. **45**, 283 (1997); (d) V. Marvaud, J. M. Herrera, T. Barilero, F. Tuyeras, R. Garde, A. Scuiller, C. Decroix, M. Cantuel, C. Desplanches. In *Molecular Magnets: Recent Highlights*, W. Linert and M. Verdaguer (Eds.), p. 33, Springer, Wien (2003).
4. See, for example: (a) M. Pilkington and S. Decurtins. In *Magnetism: Molecules to Materials II*, J. S. Miller and M. Drillon (Eds.), p. 339, VCH, Weinheim (2001); (b) O. Costisor, K. Mereiter, M. Julve, F. Lloret, Y. Journaux, W. Linert, M. Andruh. *Inorg. Chim. Acta* **324**, 352 (2001); (c) G. Marinescu, D. Visinescu, A. Cucos, M. Andruh, Y. Journaux, V. Kravtsov, Yu. A. Simonov, J. Lipkovski. *Eur. J. Inorg. Chem.* 2914 (2004).
5. R. E. P. Winpenny. *J. Chem. Soc., Dalton Trans*. 1 (2002).
6. F. A. Cotton, C. Lin, C. A. Murillo. *Acc. Chem. Res.* **34**, 759 (2001).
7. (a) S. R. Batten and R. Robson. *Angew. Chem., Int. Ed.* **37**, 1460 (1998); (b) S. Kitagawa, R. Kitaura, S. Noro. *Angew. Chem., Int. Ed.* **43**, 2334 (2004); (c) M. J. Zaworotko. *Chem. Commun.* 1 (2001); (d) A. N. Khlobystov, A. J. Blake, N. R. Champness, D. A. Lemenovskii, A. G. Majouga, N. V. Zyk, M. Schröder. *Coord. Chem. Rev.* **222**, 155 (2001).
8. H. W. Roesky and M. Andruh. *Coord. Chem. Rev.* **236**, 91 (2003).
9. V. Tudor, G. Marin, V. Kravtsov, Yu. A. Simonov, J. Lipkowski, M. Brezeanu, M. Andruh. *Inorg. Chim. Acta* **353**, 35 (2003).
10. G. Marin, V. Tudor, V. Ch. Kravtsov, M. Schmidtmann, Yu. A. Simonov, A. Müller, M. Andruh. *Cryst. Growth Design* **5**, 279 (2005).
11. L. Carlucci, G. Ciani, D. M. Proserpio. *Coord. Chem. Rev.* **246**, 247 (2003).
12. D. Benkstein, J. T. Hupp, C. L. Stern. *J. Am. Chem. Soc.* **120**, 12982 (1998).
13. S. M. Woessner, J. B. Helms, Y. Shen, B. P. Sullivan. *Inorg. Chem.* **37**, 5406 (1998).
14. T. Rajendran, B. Manimaran, F. Y. Lee, G. H. Lee, S. M. Peng, C. M. Wang, K. L. Lu. *Inorg. Chem.* **39**, 2016 (2000).
15. D. Visinescu, M. Andruh, A. Müller, M. Schmidtmann, Y. Journaux. *Inorg. Chem. Commun*. **5**, 42 (2002).
16. D. Visinescu. G. I. Pascu, M. Andruh, J. Magull, H. W. Roesky. *Inorg. Chim. Acta* **340**, 210 (2002).
17. D. Visinescu, A. M. Madalan, V. Kravtsovm, Yu. A. Simonov, M. Schmidtmann, A. Müller, M. Andruh. *Polyhedron* **22**, 1385 (2003).

18. G. S. Papaefstathiou, Z. Zhong, L. Geng, L. R. MacGillivray. *J. Am. Chem. Soc.* **126**, 9158 (2004).
19. M. Pascu, M. Andruh, A. Müller, M. Schmidtmann. *Polyhedron* **23**, 673 (2004).
20. M. Pascu, F. Lloret, N. Avarvari, M. Julve, M. Andruh. *Inorg. Chem.* **43**, 5189 (2004).
21. H. Oshio and H. Ichida. *J. Phys. Chem.* **99**, 3294 (1995).
22. J.-P. Costes, F. Dahan, A. Dupuis, J. P. Laurent, *Inorg. Chem.* **35**, 2400 (1996).
23. R. Gheorghe, M. Andruh, A. Müller, M. Schmidtmann. *Inorg. Chem.* **41**, 5314 (2002).
24. R. Gheorghe, M. Andruh, J.-P. Costes. B. Donnadieu. *Chem. Commun.* 2778 (2003).
25. A. Figuerola, C. Diaz, J. Ribas, V. Tangoulis, J. Granell, F. Lloret, J. Mahía, M. Maestro. *Inorg. Chem.* **42**, 641 (2003).
26. A. M. Madalan, H. W. Roesky, M. Andruh, M. Noltemeyer, N. Stanica. *Chem. Commun.* 1638 (2002).